

# INTERNATIONAL SOCIETY FOR SOIL MECHANICS AND GEOTECHNICAL ENGINEERING



*This paper was downloaded from the Online Library of the International Society for Soil Mechanics and Geotechnical Engineering (ISSMGE). The library is available here:*

<https://www.issmge.org/publications/online-library>

*This is an open-access database that archives thousands of papers published under the Auspices of the ISSMGE and maintained by the Innovation and Development Committee of ISSMGE.*

# Effects of plane shapes of a cofferdam on 3D seepage failure stability and axisymmetric approximation

Effets des formes planes d'un batardeau sur la stabilité après une rupture par infiltration tridimensionnelle et sur l'approximation axisymétrique

Tanaka T., Kusumi S., Inoue K.

*Department of Agricultural and Environmental Engineering, Kobe University, JAPAN*

**ABSTRACT:** In the excavation of soil with a high ground water level, seepage failure is often a problem. For excavations over a large area, seepage failure is a problem in two dimensions. In contrast, the more the region of a cofferdam is restricted, the greater the seepage flow concentrates three-dimensionally. This three-dimensionally concentrated flow lowers the safety factor for seepage failure more than under the two-dimensional condition. In this paper, seepage failure experiments were conducted under three-dimensional flow conditions for various cases of penetration ratios of sheet piles and analyses of FEM seepage flow and stability against the seepage failure of soil were carried out using the Prismatic failure concept 3D. The critical hydraulic head differences obtained by experiments and the theoretical values are examined for several cases. Effects of plane shapes of a cofferdam on the theoretical critical hydraulic head differences and axisymmetric modeling of three-dimensional seepage failure are also discussed.

**RÉSUMÉ :** Dans le cas de l'excavation d'un sol où le niveau des eaux souterraines est élevé, la rupture par infiltration constitue souvent un problème. Lorsque l'excavation est effectuée sur une grande surface, la rupture par infiltration devient alors un problème en deux dimensions. En revanche, plus la zone du batardeau est limitée, plus le flux d'infiltration se concentre en trois dimensions. Or, comparé à ce qui se passe dans un contexte bidimensionnel, ce flux concentré de manière tridimensionnelle réduit davantage le facteur sécurité lié à une rupture par infiltration. Dans cet article, nous décrivons les expériences sur la rupture par infiltration menées dans les conditions d'un flux tridimensionnel pour divers ratios de pénétration dans des palplanches. Nous y rapportons aussi les analyses du flux d'infiltration et de la stabilité suivant le modèle FEM par rapport à la rupture par infiltration du sol, menées à l'aide d'un concept prismatique de rupture en trois dimensions. Nous avons examiné, pour plusieurs cas, les rapports de niveau hydraulique obtenus dans les expériences et la théorie. Les effets des formes planes d'un batardeau sur les rapports de niveau hydraulique critiques d'ordre théorique et la modélisation axisymétrique de la rupture par infiltration tridimensionnelle y sont également évoqués.

**KEYWORDS:** three dimensional seepage failure (3DSF), surface shape of a cofferdam, axisymmetric modeling of 3DSF

## 1 INTRODUCTION

In the excavation of soil with a high ground water level, sheet piles or diaphragm walls are often used to retain soil and water. Under such conditions, seepage flow occurs through the soil, and seepage failure is often a problem. For excavations over a large area, seepage failure is a problem in two dimensions. In contrast, the more the region of a cofferdam is restricted and the deeper the penetration of the sheet piles, the greater the seepage flow concentrates three-dimensionally within it. The three-dimensionally concentrated flow lowers the safety factor for seepage failure more than under the two-dimensional condition (Nikkei construction, 2001). Such a case must be treated in three dimensions.

In this paper, seepage failure experiments were conducted under three-dimensional flow conditions for various cases of total depths of soil,  $T$ , and penetrated depths of sheet piles,  $D$ , with a plane shape of a cofferdam of 1:2. Analyses of FEM seepage flow and stability against the seepage failure of soil were carried out using the Prismatic failure concept 3D. The hydraulic head differences at deformation in the experiment,  $H_p$ , and theoretical critical hydraulic head differences based on the Prismatic failure concept 3D,  $H_c$ , are examined for the same cases. The theoretical critical hydraulic head differences for various plane shapes of a cofferdam, e.g., short to long length of 1:1, 1:2, 1:3, and 1:4, were calculated, and the effects of plane shapes of a cofferdam on the theoretical critical hydraulic head differences are discussed. The axisymmetric modeling of three-dimensional seepage failure is also discussed.

## 2 THREE DIMENSIONAL EXPERIMENTS

### 2.1 Test apparatus

A test apparatus was designed to study 3D seepage failure of soil within a cofferdam as shown in Figure 1. In the experiment, one quarter of the three dimensional region is examined. The seepage tank is made of stainless steel, 1,000mm wide, 1,300mm high and 1,000mm deep. The front of the tank is made of transparent glass for observation of the behavior of soil particles inside and the right side of the tank is equipped with 283 piezometer holes for the measurement of pore water pressures. A cofferdam is mounted on the right/front side with surface size 200mm×400mm. Seepage water flows through a sand model under the difference in water head  $H$  between the downstream water level at the top of the right-hand-side drainage hole and the upstream water level kept constant by the constant-head device.

### 2.2 Test material and test cases

In seepage failure experiments, uniform fine sand (Lake Biwa Sand 3: under 850 $\mu$ m mesh, 50% grain size  $D_{50}$ =0.283 mm, specific gravity  $G_s$ =2.67 and uniformity coefficient  $U_c$ =1.40) was used. Seventeen tests E0301 to E0317 were conducted. The following notation is used:  $T_1$  and  $D_1$  are the total depth of soil and penetration depth of sheet piles on the upstream side,  $T$  and  $D$  are those on the downstream side,  $d$  ( $=D_1-D$ ) is the excavation depth for the excavation model, and  $D_r$  is the relative density of soil. For a no-excavation model,  $T_1=T$ ,  $D_1=D$  and  $d=0$  are applied.

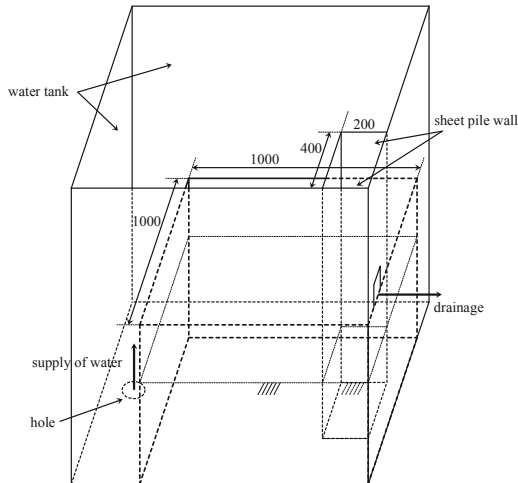


Figure 1. Schematic sketch showing test apparatus

### 3 EXPERIMENTAL RESULTS

#### 3.1 $H-Q_{15}$ curve and change in shapes of soil surface

Figure 2 shows the  $H-Q_{15}$  curve for test E0317, where  $Q_{15}$  is the discharge at 15 degrees Centigrade. It is observed from Figure 2 that  $Q_{15}$  increases linearly with increasing  $H$  until a certain value  $H_d$ .  $H_d$  value is referred to as the hydraulic head difference at which the  $H-Q_{15}$  curve diverts from linearity. As stated below, at almost the same point as  $H_d$ , the soil surface begins to settle on the upstream side and rise on the downstream side. This is because, just at this point, the soil loosens on the downstream side, the void space enlarges, permeability of the soil grows larger, and discharge increases non-linearly with  $H$ . As  $H$  increases beyond  $H_d$ ,  $Q_{15}$  becomes larger with increasing  $H$  more steeply than before, and the ground finally collapses at the hydraulic head difference at failure  $H_f$ .

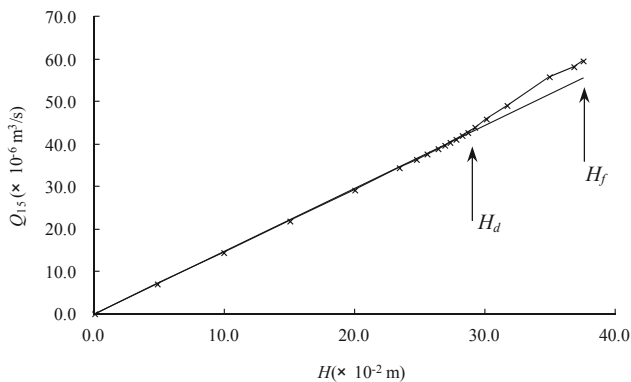


Figure 2.  $H-Q_{15}$  curves for test E0317

The heights of the soil surface are measured at several chosen points along the measurement line shown in Figure 3. The measurement line is a bisector of the right angle of the inside corner of the rectangular diaphragm wall. Figures 4 (a)-(c) show the changes in shape of the surface of the sand model along the surface height measurement line with increase in  $H$ , from  $H=4.81$ cm at the first step to  $H=36.78$ cm at one step before failure. The model sand is in a stable state at early steps of  $H$  (Figure 4(a)). When  $H$  increases beyond a certain value  $H_y$ , the model sand changes in shape near the sheet pile wall. The surface of the soil in the vicinity of the sheet pile wall subsides on the upstream side and rises on the downstream side (Figure 4(b)). The value of  $H_y$  is referred to as the hydraulic head difference at onset of deformation. It was found from a series of

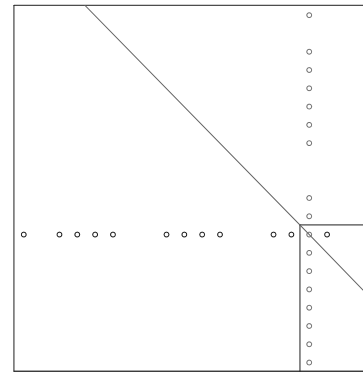
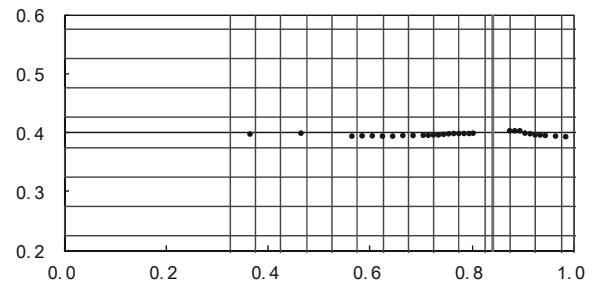
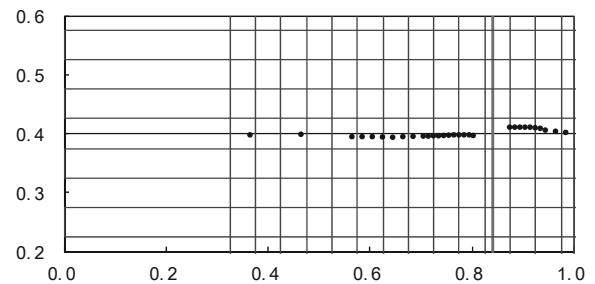


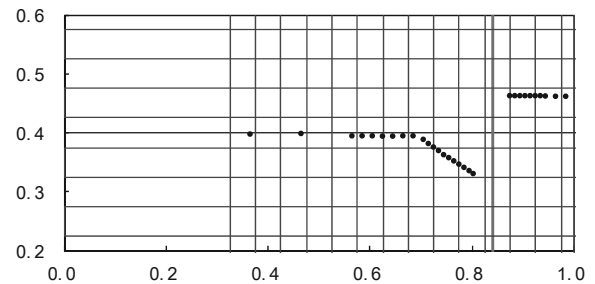
Figure 3. Measurement line of the height of soil surface



(a) At the early step of  $H$  ( $H=4.81$ cm)



(b) At the  $H$  value just beyond  $H_y$  ( $H=30.06$ cm)



(c) At the one step before failure ( $H=36.78$ cm)

Figure 4. Changes in shape of surface of sand model along the surface height measurement line with increase in  $H$



Figure 5. A close-up photo of the upstream inverse conical shape at  $H=36.78$ cm (E0317)

tests that the experimental results lead to the interesting conclusion  $H_y = H_d$ .

Subsidence of the upstream soil surface and rising of the downstream soil surface proceed with steps of increasing  $H$ . The upstream soil surface is an inverse conical shape centered at the outer corner of the rectangular diaphragm wall. A close-up photo of the upstream inverse conical shape is shown in Figure 5 at  $H=36.78\text{cm}$  (E0317). The rise in the downstream soil surface occurs uniformly within a certain width from the sheet pile wall. As  $H$  increases and approaches  $H_f$ , the upstream subsidence shows a clear inverse conical shape, and sand particles are observed to roll down the slope of the upstream soil surface (Figure 4 (c)).

#### 4 STABILITY ANALYSES –RESULTS AND DISCUSSIONS–

##### 4.1 Prismatic failure concept 3D

The Prismatic failure concept 3D presented by Tanaka et al. (2012) is used for estimating the stability against seepage failure of soil. In the Prismatic failure concept 3D, we assume that the body of soil lifted by seepage water has the shape of a prism with a certain height and width adjoining the sheet pile wall. The rise of the prism is resisted by the submerged weight,  $W'$ , and frictions  $F_{RL}$  and  $F_{RCR}$  on the left and right sides and  $F_{RF}$  and  $F_{RCB}$ , on the front and back sides. The safety factor  $F_s$  with respect to the rise of the prism, which is subjected to the excess pore water pressure on its base,  $U_e$ , is given as:

$$F_s = \frac{W' + F_{RL} + F_{RCR} + F_{RF} + F_{RCB}}{U_e} \quad (1)$$

For the hydraulic head difference  $H$  between up- and downstream sides, safety factors,  $F_s$ , are calculated for all of the prisms within a cofferdam. The safety factor  $F_s$  takes the minimum  $F_{s\min}$  for a certain prism among all of the prisms. The calculation is iterated for another hydraulic head difference,  $H$ , until the condition whereby  $F_{s\min}$  becomes nearly equal to 1.0 is found.  $H=H_c$  at which the condition  $F_{s\min}=1.0$  is applied is defined as the critical hydraulic head difference. The prism with a value of  $F_{s\min}=1.0$  among all of the prisms for  $H=H_c$  is defined as the critical prism. We could say that the critical prism is separated from the underlying soil at its base when  $H$  exceeds  $H_c$ . Safety factors using the Prismatic failure concept 3D when considering frictions are discussed below.

##### 4.2 Relationship between hydraulic head differences $H_c$ (by theory) and $H_y$ (by experiment)

For Lake Biwa sand 3 of  $D_r=50\%$ , the theoretical hydraulic head difference by the Prismatic failure concept 3D,  $H_{PF}$  [Tanaka et al. 2012] is analyzed taking the anisotropy of the test sand to be  $k_{xy}/k_{zz}=1.20$  [Tanaka et al. 2011]. Figure 6 shows the relationship between  $D/T$  and  $H_c\gamma_w/T\gamma'$  for a no-excavation model. The experimental results are also plotted in Figure 6. It is observed from Figure 6 that the calculated critical hydraulic head differences  $H_{PF}$  are very close to the measured  $H_y$ . The Prismatic failure concept 3D thus proved to be a useful method for calculating critical hydraulic head difference at the onset of deformation of soil within a cofferdam. The same is true of the excavation model.

##### 4.3 Effects of surface shape of a cofferdam on $H_c$

Let us consider a cofferdam whose surface shape is rectangular with the shorter length at  $B$  and longer length at  $L$  (see Figure 7). Four cases of  $B:L=1:1, 1:2, 1:3$  and  $1:4$  are analyzed for constant values of  $B=0.2\text{m}$  and  $W=0.8\text{m}$ . Figure 8 shows the relationship between  $D/T$  and  $H_c\gamma_w/T\gamma'$ . It follows from Figure 8 that:

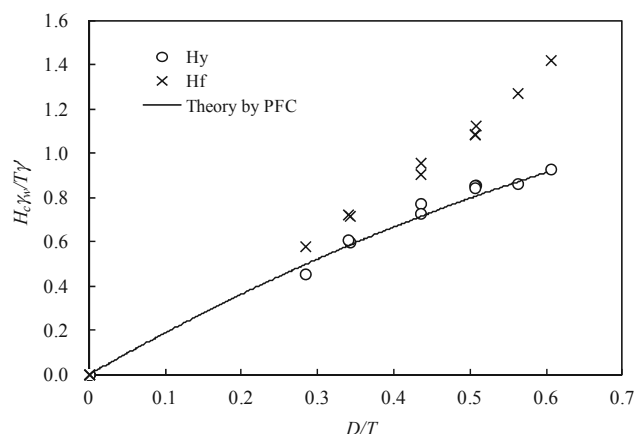


Figure 6. Relationship between  $D/T$  and  $H_c\gamma_w/T\gamma'$  for no excavation model

- (1)  $H_c$  gives the lowest value in the case of 1:1.
- (2) For the same value of penetration ratio of sheet piles,  $D/T$ , the critical hydraulic head differences,  $H_c$ , are given as follows in order of increasing magnitude:  $1:1 < 1:2 < 1:3 < 1:4$ .
- (3) For the same value of a short length, the more the longer length increases, the smaller the effect of the longer length on  $H_c$  becomes.  $H_c$  in the case of 1:3 almost equals the  $H_c$  in the case of 1:4 for the same value of  $D/T$ .
- (4) For a small value of  $D/T$ , all of the  $H_c$  values are nearly equal in cases of 1:1, 1:2, 1:3, and 1:4.

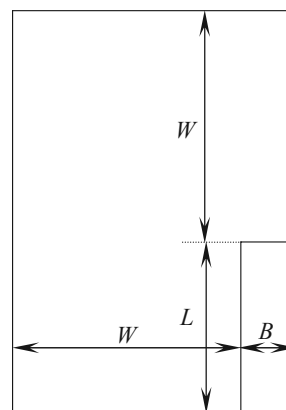


Figure 7. Plane shape of a cofferdam

#### 5 AXISYMMETRIC MODELING OF THREE-DIMENSIONAL SEEPAGE FLOW

In the experiment, one quarter of the three dimensional region is examined as stated earlier. The surface shape of the cofferdam is rectangular with the shorter length at 1 and longer length at 2. Considering an inscribed circle in the shorter side of the rectangle as shown in Figure 9, an axisymmetric seepage flow through the soil is used to model such a three-dimensional flow.

Let us consider the three dimensional and approximate axisymmetric conditions:  $T=40\text{cm}$ ,  $D=20\text{cm}$  and  $R=20\text{cm}$  for the non-excavation sand models, where  $R$  is the radius of the circular wall in the axisymmetric condition. Figure 10 shows the relationship between the penetration ratio of sheet piles  $D/T$  and the non-dimensional value of  $H_c$ ,  $H_c\gamma_w/T\gamma'$ . It is found from Figure 10 that the three dimensional seepage failure phenomena are well approximated using axisymmetric seepage failure. For further details, the following points may be made:

- (1)  $D/T \leq 0.40$   $H_c$  values are larger in the AXS flow than in the 3D flow; in particular the approximate accuracy with respect to  $H_c$ ,  $(H_{c\text{AXS}} - H_{c\text{3D}})/H_{c\text{3D}}$ , is about +17% for  $D/T = 0.27$ . This

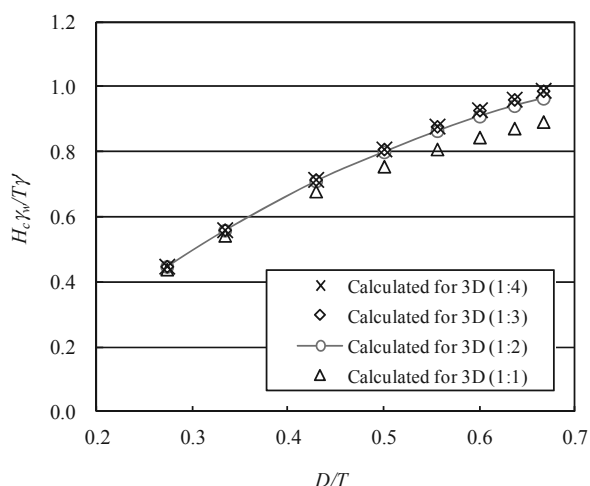


Figure 8. Relationships between  $D/T$  and  $H_c\gamma_w/T\gamma'$  for various plane shapes

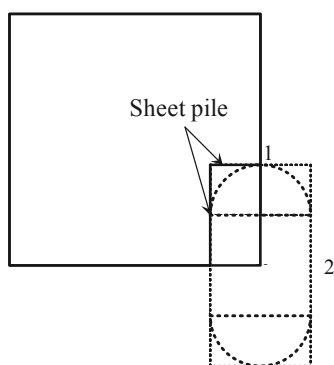


Figure 9. Plane figure of the 3D test apparatus (axisymmetric modeling)

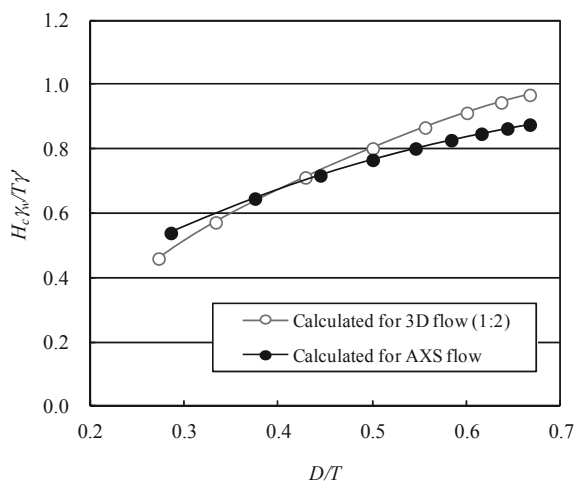


Figure 10. Relationship between  $D/T$  and  $H_c\gamma_w/T\gamma'$  (Axisymmetric modeling of 3D flow)

means that assuming that the 3D flow is the same as AXS flow leads to an overestimation of  $H_c$ , and generates unreasonable results with respect to seepage failure.

(2)  $D/T > 0.40$   $H_c$  values are smaller in the axisymmetric case than in the three-dimensional case; the approximate accuracy,  $(H_{c\text{ AXS}} - H_{c\text{ 3D}})/H_{c\text{ 3D}}$ , is about  $-9\%$  for  $D/T = 0.67$ . This means that assuming that the 3D flow is the same as AXS flow leads to an underestimation of  $H_c$ , and generates uneconomical designs with respect to the  $H_c$  value.

For the same value of  $D/T$ , the  $H_c$  values are given as follows in order of increasing magnitude:  $B:L = 1:1 < 1:2 < 1:3 < 1:4$  as stated in Section 4.3. The same axisymmetric approximation is

applied in these four cases. So, the difference in  $H_c$  between 3D and AXS flows changes, and the approximate accuracies,  $(H_{c\text{ AXS}} - H_{c\text{ 3D}})/H_{c\text{ 3D}}$ , are given as  $-2\%$  (1 : 1),  $-9\%$  (1 : 2),  $-11\%$  (1 : 3) and  $-12\%$  (1:4) for  $D/T = 0.67$ .

## 6 CONCLUSIONS

Seepage failure experiments were conducted under three-dimensional flow conditions for various cases of total depths of soil,  $T$ , and penetrated depths of sheet piles,  $D$ , and analyses of FEM seepage flow and stability against the seepage failure of soil were carried out using the Prismatic failure concept 3D (pfc 3D). From discussions, the following results were obtained:

(1) With an increase in the hydraulic head difference between up- and downstream,  $H$ , the discharge at  $15^\circ\text{C}$ ,  $Q_{15}$ , increases linearly for a smaller value of  $H$ , but changes abruptly and non-linearly beyond the point  $H=H_d$ .  $H_d$  is referred to as the hydraulic head difference at an abrupt change of the  $H-Q_{15}$  curve.

(2) In correlation with the above phenomenon regarding the  $H$  and  $Q_{15}$  relationship, the height of the soil surface changes at the front (downstream) and rear (upstream) of the sheet piles. When  $H$  increases beyond  $H_y$ , a downstream rise and upstream drop of the soil surface occur.  $H_y$  is referred to as the hydraulic head difference at the onset of soil deformation.

(3) Sand particles move from up- to downstream sides under the bottom edges of the sheet piles. The upstream soil surface is an inverse conical shape centered at the outer corner of the rectangular diaphragm wall.

(4) The experimental results led to the interesting conclusion that  $H_y=H_d$ .

(5) The hydraulic head differences at deformation in the experiment,  $H_y (=H_d)$ , are nearly equal to the theoretical critical hydraulic head differences based on the pfc 3D,  $H_c$ .

The theoretical critical hydraulic head differences for various plane shapes of a cofferdam, e.g., a short to long length of 1:1, 1:2, 1:3, and 1:4, were calculated, and the following results were obtained:

(6)  $H_c$  gives the lowest value in the case of 1:1.

(7) For the same value of the penetration ratio of sheet piles,  $D/T$ , the critical hydraulic head differences,  $H_c$ , are given as follows in order of increasing magnitude:  $1:1 < 1:2 < 1:3 < 1:4$ .

(8) For the same value of a short length, the more the longer length increases, the smaller the effect of the longer length on  $H_c$  becomes.  $H_c$  in the case of 1:3 almost equals the  $H_c$  in the case of 1:4 for the same value of  $D/T$ .

(9) For a small value of  $D/T$ , all of the  $H_c$  values are nearly equal in cases of 1:1, 1:2, 1:3, and 1:4.

The axisymmetric modeling of three-dimensional seepage failure was discussed, concluding as follows:

(10) With respect to the seepage failure problem, axisymmetric seepage flow through soil within a cylindrical wall can be used to model such a three-dimensional flow. The magnitudes of the critical hydraulic head differences  $H_{c\text{ 3D}}$  (in three dimensions) and  $H_{c\text{ AXS}}$  (axisymmetric model) are given as follows for the 3D case of 1:2 and its axisymmetric model:  $H_{c\text{ 3D}} < H_{c\text{ AXS}}$  for  $D/T \leq 0.40$ , and  $H_{c\text{ 3D}} > H_{c\text{ AXS}}$  for  $D/T > 0.40$ .

## 7 REFERENCES

Nikkei Construction. 2001. Shortage of penetration depth of sheet piles, Nikkei Business Publications, 37-38, 2001.9.28.  
 Tanaka T., Naganuma H., Shinha M., Kusumi S. and Inoue K. 2011. Anisotropic permeability of soil on 3D seepage failure experiments, *Procs. of the 68th annual meeting of the Kyoto Branch of Japanese Society of Irrigation, Drainage and Rural Engineering*, 3-5 - 3-6.  
 Tanaka T., Hirose D. and Kusumi S. 2012. Seepage failure of sand within a cofferdam in three dimensions -Prismatic failure concept 3D and analytical consideration-, *Report of Research Center for Urban Safety and Security*, Kobe University, No.12, 285-299.